Technical Report

Department of Computer Science
and Engineering
University of Minnesota
4-192 Keller Hall
200 Union Street SE
Minneapolis, MN 55455-0159 USA

TR 19-008

UAV Landing at an Unknown Location Marked by a Radio Beacon

Nikolaos Stefas, Haluk Bayram, Volkan Isler

July 30, 2019

Revised

UAV Landing at an Unknown Location Marked by a Radio Beacon

Nikolaos Stefas, Haluk Bayram and Volkan Isler
University of Minnesota *

Abstract

We consider the problem of minimizing the time to approach and land near a target radio beacon at an unknown location with an Unmanned Aerial Vehicle (UAV). We show that a cone-like region exists above the target inside of which bearing measurements of a directional antenna lose directionality: signal recordings in all directions yield similar signal strength. We present a geometric model of this region based on antenna simulations and data collected with a real system. Our main contribution is a strategy that takes advantage of a UAV's ability to change altitude and exploits a special structure occurring when approaching the target beacon from above to reduce the flight time required to land near the beacon. We analyze the performance of our strategy and demonstrate through simulations that by exploiting this structure we can achieve shorter flight times than our previous work.

1 Introduction

Landing near the source of radio signal (beacons) with Unmanned Aerial Vehicles (UAVs) has many important applications. In search and rescue applications, beacons can mark the location of an emergency package delivery like rations and medicine [1], defibrillators [2] and flotation devices [3]. In environmental monitoring applications, radio-tagging animals can be used to mark their location [4], [5] and can be a useful wildlife and farm management tool. UAVs equipped with a directional antenna that can track radio beacons are a good fit in such scenarios due to their ability to travel fast, reach difficult to access areas and carry small payloads.

A common technique to locate the area of a target radio beacon using directional antennas is the triangulation of bearing measurements [6, 7, 8]. There are primarily two ways of obtaining bearing measurements (directionality). We can either use a single directional antenna or use omnidirectional, multi-array antennas. In this work we focus on a single directional antenna. Bearing measurements in this case are acquired by rotating the antenna

*This work is supported in part by MnDRIVE, NSF awards #1525045 and #1617718 and MN LCCMR. H. Bayram is also supported by TUBITAK 2232 (#119C008). Stefas and Isler are at the University of Minnesota. Bayram is at Istanbul Medeniyet University. Emails : stefa125@umn.edu, isler@umn.edu, haluk.bayram@medeniyet.edu.tr

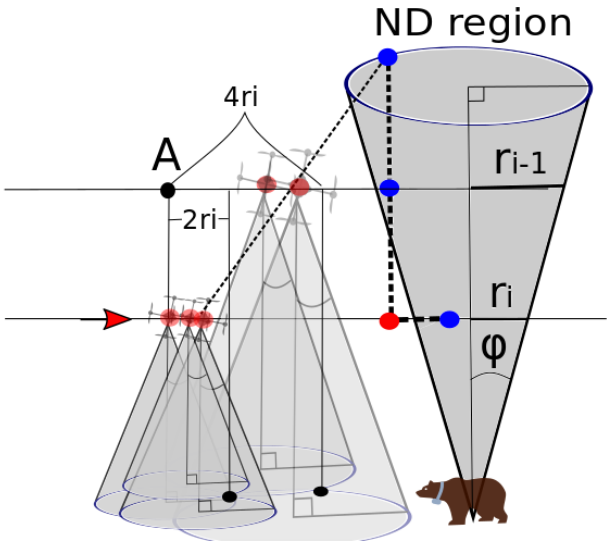

Figure 1: A UAV may be unable to localize a radio beacon with a directional antenna at a high altitude due to the existence of a cone-like region above the target inside of which we lose directionality. We name this region No Directionality (ND) region and present a strategy that utilizes uses binary measurements to detect it (red if outside, blue if inside). We first detect the ND region by increasing the height and covering an increasing area around the starting location A. Then we reduce the uncertainty area by lowering the height and reducing the size of the ND region so that $r_i < r_{i-1}$ and re-locating it.

in place with a fixed angle step and selecting the direction that recorded the strongest signal [9]. Due to multi-path effects and interference in unknown environments we cannot assume that the signal strength monotonically increases as we approach the beacon and a full rotation is required to normalize the recordings [10]. The duration of a bearing measurement depends on the angle step and the beacon's number of pulses per second. For example, a bearing measurement of angle step 10 deg and a beacon transmitting signals at 0.5 Hz requires over a minute to complete. A UAV able to reach an 18 m/s speed can travel over 1000 m during that time. In many UAV systems the time spent acquiring bearing measurements can be orders of magnitude larger than travel time [11].

In this work we take advantage of a UAV's ability to change altitude and exploit a special structure occurring when approaching the target beacon from above to significantly reduce measurement acquisition time (Figure 1). Many studies have used UAVs with directional antennas in order to determine the area a target beacon lies in [11], [12], [13]. However in most cases the altitude is fixed and the target is not approached from above. Reducing measurement acquisition time has been studied recently in [10] where a directional and omni-directional antennas are used together to remove the need of full rotation bearing measurements for signal strength normalization. However, the authors do not provide any mathematical guarantees for localization time and their approach does not take advantage of a UAV's ability to change altitude. We show that there exists a region above the target inside of which bearing measurements with a directional Yagi antenna lose directionality: signal recordings in all directions yield similar signal strength. We name this region *No Directionality* (ND) region. We also show that we can detect whether a location is inside

the region (binary ND measurement) with only four signal recordings. The authors in [14] mention this region but they explicitly avoid it because their approach can fail when near the region. Using this special structure we provide a strategy for UAVs to land near a target beacon using only one initial bearing measurement and ND measurements.

Our contributions can be summarized as follows:

1. We present a strategy that exploits a special structure occurring when approaching the target beacon from above. Our strategy takes advantage of a UAV's ability to change altitude and utilizes this special structure to reduce the flight time required to land near the beacon.

2. We analyze the strategy performance and show through simulations that in comparison to our previous work it can reduce the time it takes for a UAV to localize and land near the target and validate it on a real system.

2 Problem Statement

Our problem, No Directionality (ND) region-based target landing can be formulated in the following way. We are given an initial measurement angle (bearing) corrupted with an upper bounded noise α and an approximation of the ND region of a stationary signal transmitter as being perceived by the receiver. The goal is for a UAV to land on a target area of radius r^* such that the total (flight) time is minimized:

$$\min_{S} time(S) = \frac{1}{\|v\|} \sum_{i=1}^{N-1} \|s_i, s_{i+1}\| + N\tau_m \tag{1}$$

$S = \{s_1, ..., s_N\}$ is the set of measurement locations, $\|v\|$ is the robot speed which we assume to be constant, $\|s_i, s_{i+1}\|$ is the distance between locations s_i, s_{i+1} and τ_m is the (fixed) time required for taking a single measurement. Since the target beacon is assumed to be stationary, the landing location does not change over time. We also assume that the signal can be sensed at all times, if not we can just search for it.

3 No-Directionality Region Modeling

In this section we model the area around the target beacon based on our antenna radiation field and classify the locations in which we can or cannot obtain reliable directionality measurements. Our antenna operates at the 163 MHz range with a director of 0.84 m length and 0.25 m spacing, an exciter of length 0.88 m and a reflector of 0.93 m length and 0.26 m spacing. Using the Matlab antenna toolbox we obtained the electrical field strength around the antenna for multiple angles corresponding to different locations relative to the target beacon. For each location we obtained the relative field strength by rotating the antenna in place while keeping it horizontal with respect to the ground plane. In Figure 2 we present the electrical field strength for two sample locations. The relative field strength drops as we increase the altitude and it becomes increasingly difficult to determine the direction to the signal source.

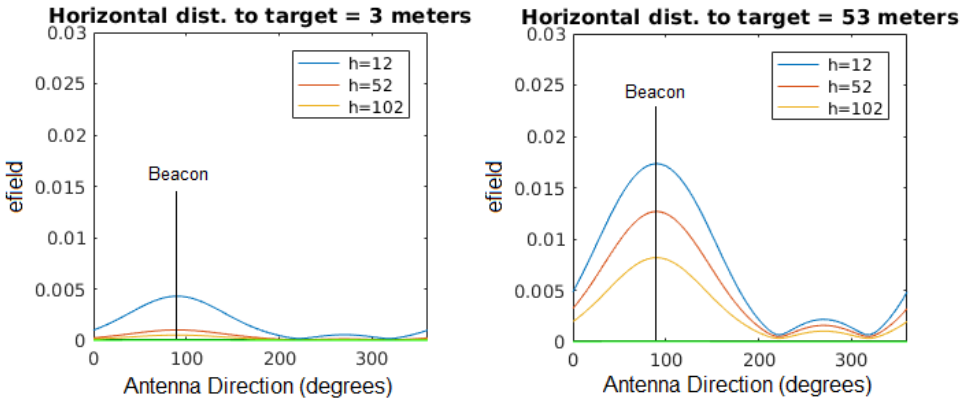

Figure 2: We observe that for a given altitude the normalized ideal signal strength flattens out as we approach the target. The electrical field strength shown is an example from two antenna locations relative to the target beacon for varying altitudes h. We use this observation to detect whether we are close to the target when at a high altitude.

We use this observation and classify locations based on whether direction to the signal source is reliable. In Figure 3 we present the results of this classification for various distances $\in \{1, 3, ..., 71\}m$ and altitudes $\in \{1, 3..., 109\}m$. For each location we obtain four signal strength values, each with a rotation of 90 deg. A location is labeled "GD" if it provides good directionality, where the difference between maximum and minimum field strength is above $threshold = 0.0054$ chosen empirically based on the real data collection. Otherwise, the location is labeled as "ND" for no directionality. For each location we obtained the results for varying angles between the antenna facing direction and direction to the source $\in \{5, 15, 25, 35, 45\}$ deg. The choice of obtaining four signal strength values results in some of the boundary locations being ambiguous labeled both as ND and GD. We obtain the boundary line(s) by calculating the largest and smallest angles between the target location and these ambiguous boundary locations. The result resembles a cone. We refer to this conic approximation of the ND region as the ND cone with apex angle ϕ. Our modeling concludes that for $SNR = 20$ there is a region (blue) with angle $\phi \in (16.7, 20.3)$ deg inside of which we cannot determine directionality. Furthermore, there exists an ambiguous region (red and blue) with angle $\theta \in (7.1, 15.4)$ deg inside of which the locations can yield both ND and GD measurements.

In order to verify that our ND region modeling is useful we collected data with a real UAV system (described in Section 6). Due to practical limitations we focused on a smaller area and used a larger grid size. The data were collected for distances $\in [9, 25]m$ and altitudes $\in [19, 44]m$. The initial direction between the first recording of each set differed by 40 deg, which yields the highest possible angle difference. The angles calculated using the real data were $\phi = 17.8$ deg, $\theta = 17.4$ deg. These results resemble the noisy simulated case and indicate that our modeling can be of practical use.

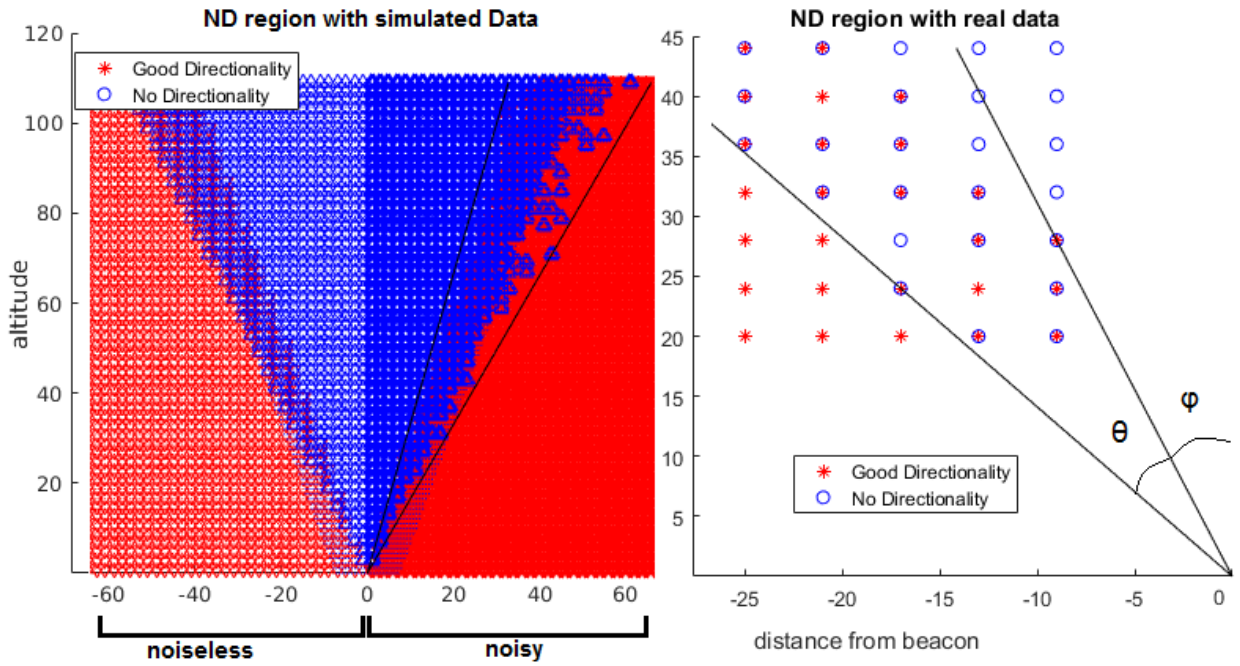

Figure 3: Classifying locations on whether they provide good directional measurements (GD, red) or not (ND, blue) based on expected electrical field strength. The resulting approximation resembles a cone (blue area) of apex angle ϕ. At the boundaries of the cone there exists an ambiguous area of angle θ containing both ND and GD locations. The ND region with simulated data plot represents two cases. First, the noiseless case where $\phi = 20.3$, $\theta = 7.1\,\text{deg}$. Second, adding white Gaussian noise with $SNR = 20$ results in $\phi = 16.7$, $\theta = 15.4\,\text{deg}$. The ND region with real data plot was created with data collected with a real UAV system and resulted in $\phi = 17.8$, $\theta = 17.4\,\text{deg}$.

4 Strategy

The strategy can be seen in Algorithm 1 and relies on the conic approximation of the ND region presented in Section 3. Other than the initial bearing measurement, we only use binary ND measurements that are much faster and can detect whether we are inside the ND region. Taking an ND measurement at height H_i, we can determine whether the target's ground location is within radius $r_i = H_i \tan \phi$ from the measurement ground location.

Our strategy is split into two phases (see Figure 1) : The goal of the first phase is to ensure the ND region is detected. At the beginning of Phase 1 there are two possibilities, either the ND region can be detected at the initial location A or not. If at location A we do not detect the ND region, then we take more ND measurements at locations near A and towards the direction of the initial bearing measurement (blue circles in Figure 4). If the target is not inside the area covered by these measurements, we increase the altitude such that the ND measurement footprint increases and covers a larger area (red circles in Figure 4). This is repeated until the ND region is detected.

The goal of the second phase is to ensure that the radius of the ND region is at most r^*. At the end of Phase 1 we have entered the ND region but its radius at its current height may be larger than r^*. In this case Phase 2 reduces height and follows the boundary of the ND region until its radius reduces to at most r^*. If at any point during Phase 2 we exit the ND region while reducing height, then we re-detect it. Re-detecting the ND region is similar to Phase 1 but since we no longer know its direction, we obtain ND measurements in all directions.

The inputs to Algorithm 1 are desired landing area radius r^*, direction of the initial bearing measurement, initial starting location A, ND cone apex angle ϕ and bearing measurement noise α. In order to provide performance guarantees in terms of task completion we get the competitive ratio with respect to the optimal offline strategy outlined in Section 4.1. The details of the performance analysis for Phase 1 and Phase 2 while $\theta = 0$ is provided in Sections 4.2 and 4.3 and complete proofs are included in the appendix. Then we address the case where $\theta > 0$ in Section 4.4.

Algorithm 1 `ND-Region-Landing`

Input: r^*, A, ϕ, α, Initial bearing
Output: Landing location s_N
1: Call Algorithm 2 to detect the ND region
2: Call Algorithm 3 to reduce ND region radius to r^* and determine the landing location s_N

4.1 Lower Bounding the Optimal Offline Strategy

For our analysis we upper bound the cost of the optimal offline algorithm OPT which has access to the target location and use this bound to compute the performance of our strategy with respect to OPT. Let OPT start at location A and have knowledge of the target location C and its corresponding ND region. If A is located outside the ND region then any strategy has to acquire at least one ND measurement to detect the region and determine that it is

inside the desired area of radius r^* and at height H^*. In order to obtain this measurement any strategy has to travel at least $L - r^*$, where $L = \|AC\|$. The total travel cost of OPT is $\leq L - r^*$ which for a constant and normalized travel speed $\|v\| = 1$ is equivalent to total flight time.

4.2 Phase 1: Detect the ND Region

In this section we show that Algorithm 2 is guaranteed to detect the ND region and analyze its performance in Theorem 3. In line 1 we acquire the initial bearing measurement, initialize our travel direction and determine the coverage pattern using Lemma 1. The loop in lines 2-10 doubles the ground and height step sizes and covers the circular sector of the circle centered at A with radius $2r_i$ and angle 2α.

Algorithm 2 `Phase 1:ND-Region-Detection`

Input: $r_0 = r^*$, $H_0 = \frac{r^*}{\tan\phi}$, A, ϕ, α, Initial bearing
Output: ND region detection location s_i
1: Determine the coverage pattern using Lemma 1
2: **while** ND region has not been detected **do**
3: Double radius r_i and height H_i
4: Based on the coverage pattern cover the circular sector of a circle with radius $2r_i$ with angle α
5: **end while**

The problem of covering the area of a circle with a number of smaller circles has been studied at [15]:

Lemma 1. *We need at most $q+1$ circles of radius r to cover a circular sector of radius $2r$ and angle $\leq 30q\,\text{deg}$, where $q \in \{1, 2, ..., 6\}$. We need at most seven circles of radius r to cover the entire area of a circle with radius $2r$.*

Using Lemma 1 we can upper bound the cost of each step of the while loop in Algorithm 2 in the following way.

Lemma 2. *Let the approximation of the ND region be a right angular cone with apex angle ϕ and its apex point at C such that at height H_i its cap is a circle with radius $r_i = H_i \tan\phi$. Let the initial bearing measurement location be A outside the ND region, height H_i and upper bounded angle noise $\alpha < 90\,\text{deg}$. If $AC \leq 2r_i$ then we can get inside the ND region with at most four steps of total length $\leq 8r_i$.*

The proof uses Lemma 1 for covering a $90\,\text{deg}$ circular sector (see Appendix 8.1 for details). Now we can upper bound the cost of Algorithm 2.

Theorem 3. *Let the initial bearing measurement location be A outside the ND region, height H_0 and upper bounded angle noise $\alpha < 90\,\text{deg}$. Let the approximation of the ND region be a right angular cone with apex angle ϕ and its apex point at C such that at height H_i its cap is a circle with radius $r_i = H_i \tan\phi$. Algorithm 2 can detect the ND region with a competitive ratio of $max\left(\frac{2L(4+\frac{1}{\tan\phi})}{(L-r^*)}, 4\log_2(\frac{L}{r^*})\right)$, for $r^* = r_0$ and $L = \|CA\|$.*

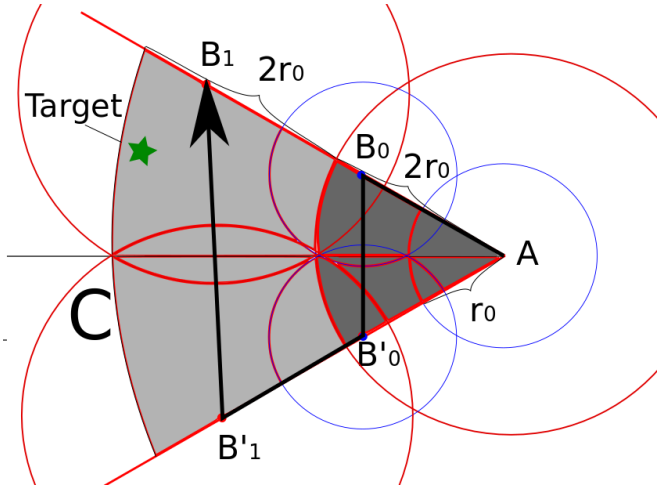

Figure 4: Detecting the ND region when the initial bearing measurement is at location A and height H_0 with bearing measurement upper bounded noise angle $\alpha = \angle B_0 A B_0'$. If the target is further away from A than $2r_0$ then the target is inside the black colored area that is the circular sector of the circle centered at A with radius $2r_0$ and angle 2α and we need at most three more ND measurements (blue circles) to cover it. If the target it is not further away than $2^{k+1}r_0$ we increase height until the radius becomes $2^k r_0$.

The proof uses the fact that if the ND region is detected at the k-th iteration then $\|CA\| = L > 2r_{k-1} = 2^k r_0$ and $k \leq \log_2(\frac{L}{r_0})$. The travel distance is upper bounded using Lemma 2 since $8\sum_{j=0}^{k} 2^k r_0 + \|H_k\| < r_0 2^k(4 + \frac{1}{\tan\phi})$. Th

4.3 Phase 2: Reduce Area of the ND Region

In this section we show that Algorithm 3 is guaranteed to reduce the ND region radius to r^* and analyze its performance. In line 1 we determine the size of the area that we need to cover and how many circles are required for a complete coverage. We will refer to the number, location and visit order of the circles as a coverage pattern. In lines 2-8 we reduce the altitude and radius of the ND conic region and attempt to detect the ND region again. In lines 4-7 we visit each circle according to the coverage pattern until we detect the ND region again. Once the radius of the ND region drops below the desired we stop and land.

At the end of Algorithm 2 the height is H_k and the last location is ensured to be inside the ND region. The goal of Algorithm 3 is to reduce the radius of the ND region to less than or equal to the desired r^*. We achieve this by lowering the height H_i such that the radius r_i of the ND region at height H_{i-1} is $r_{i-1} = \frac{r_i}{2}$. If we end up outside the ND region at height H_{i-1} then by construction we cannot be further away than $2r_{i-1}$. Since the ND region at height H_{i-1} has radius r_{i-1} we simply need to cover a circle of radius $2r_{i-1}$ with cirles of radius r_{i-1} (ND measurement coverage area).

Using Lemma 1 we can upper bound the cost of each iteration of the while loop in Algorithm 3.

Lemma 4. *Let the approximation of the ND region be a right angular cone with apex angle ϕ and its apex point at C such that at height H_i its cap is a circle with radius $r_i = H_i \tan\phi$.*

Let location A be inside the ND region at height H_i. At height $H_{i+1} = \frac{H_i}{2}$ the ND region has radius $r_{i+1} = \frac{r_i}{2}$. If location A at height $\frac{H_i}{2}$ does not lie inside the ND region then we can get inside the ND region with at most six steps (and measurements) of total length $\leq 12r_i$.

The proof is available in Appendix 8.3 and is similar to Lemma 2. Using Lemma 4 we can upper bound the cost of Algorithm 1 as follows.

Theorem 5. *Let the target beacon be at location C, the initial measurement location be A such that $\|CA\| = L$. Let the approximation of the ND region be a right angular cone with apex angle ϕ and its apex point at C such that at height H_k its cap is a circle with radius $r_k = H_k \tan\phi$. Given an initial bearing measurement of upper bounded angle noise $\alpha < 90\,\text{deg}$ Algorithm 1 can land near the target beacon within a circular area of radius r^* with a competitive ratio of $max(\frac{2L(16+\frac{2}{\tan\phi})}{(L-r^*)}, 9\log_2(\frac{L}{r^*}))$.*

The proof follows from Theorem 3 and Lemma 4. We note that for a total of m iterations the travel distance is $H_k + \sum_{j=0}^{m-1} \frac{12r_k}{2^j} \leq r_k(12 + \frac{1}{\tan\phi})$.

Algorithm 3 `Phase 2:Reduce-ND-Region-Area`

Input: r^*, $r_i = r_k$, $H_i = H_k$ ϕ, θ, α
Output: Landing location s_N

```
Determine coverage pattern based on φ, θ angles
while r_i > r* do
    Halve radius r_i and height H_i
    repeat
        Determine the next measurement location s_j based on the coverage pattern
        Go to location s_j and take ND measurement m_j
    until m_j ∈ ND region
end while
```

4.4 Handling the Ambiguous Region

In this Section we handle the existence of locations at the boundary of the ND region that may result in both good (GD) and bad (ND) directionality measurements (see Section 3). In this case Algorithm 2 may result in an early detection of the ND region. Then Algorithm 3 may miss re-detecting the ND region after reducing the altitude due to the ND region location lying further away than twice the ND region radius (Lemma 4). To address this we increase the radius of the circle we cover in Lemma 1. In other words, we handle these ambiguous locations with a simple modification of the coverage pattern in the first line of Algorithm 3. Due to the difficulty of mathematically determining the smallest number of circles of a fixed radius that cover the area of a circle of an increasing radius [16] we do not handle the general case. We only handle and analyze a few practical cases.

At height H_i the ND region can be detected at most $H_i \tan(\phi+\theta)$ away from the beacon location. This is at most $e_i = H_i \tan(\phi+\theta) - H_i \tan(\phi)$ away from the boundary of the ND cone. If we then halve the height (Algorithm 3) we can be at most $\frac{H_i}{2}\tan(\phi) + e_i = r_{i-1} + e_i$

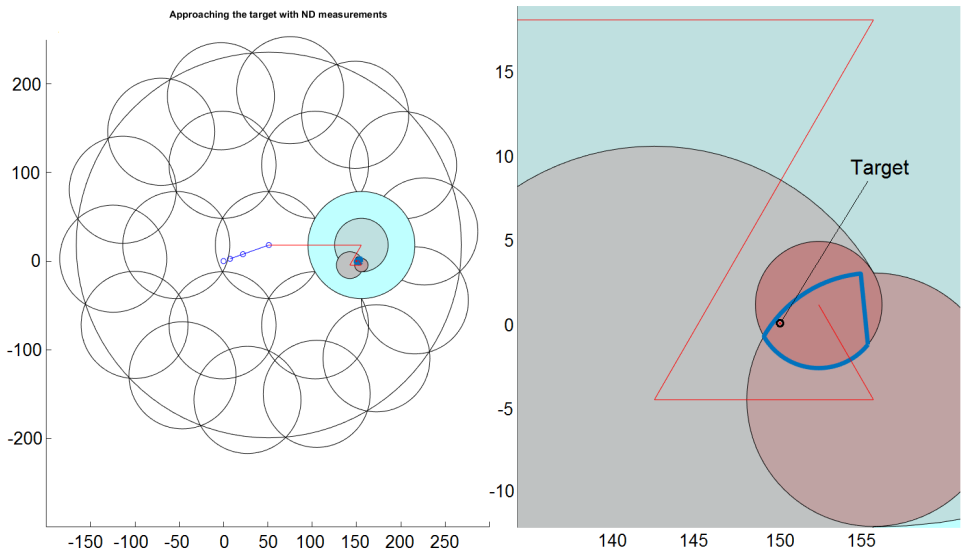

Figure 5: An example of our strategy outlined in Algorithm 1 for $\phi = 15^o$ and $\theta = 0$. The desired landing area radius is 3 m and the target beacon is located 150 m away from the starting location. The starting location is at [0,0] with an altitude of 12 m. Phase 1 (blue trajectory) detects the ND region after 4 steps at altitude 450 m. Phase 2 (red trajectory) reduces the ND region area (colored circles) until it achieves a radius of 3 m. The blue bold line is the final area uncertainty.

away from the ND region. Let $ratio = \frac{2(r_i+e_i)}{r_i}$ be the ratio between the large and small circles in the problem of covering the area of a circle with a number of smaller circles. In [17] it is shown that for ratios that are smaller than 2.246, 2.414 and 2.532 we need at most 8, 9 and 10 circles, respectively. Larger ratios are difficult to determine and require numerical evaluation [16]. In our modeling we calculated $ratio = 2$ ($\theta = 0$), $ratio < 2.9$ ($\theta = 10$) and $ratio < 3.7$ ($\theta = 17$). We can evaluate numerically that for $ratio < 2.9$ we need at most 21 circles and for $ratio < 3.3$ we need at most 48 circles. For $ratio < 3.7$ Lemma 4 requires at most 42 additional steps. This results in the cost of each step in Lemma 4 being multiplied by a factor of at most 8.

5 Simulations

In this section we show that `ND-Region-Landing` can provide short flight times when the goal is to localize and land near a target beacon. Since no other strategy considers the concept of no directionality we chose to compare the total flight times achieved by Algorithm 1 against our previously published `Localize-Target-on-Plane` algorithm [11] which chooses the location of bearing measurements during execution so as to localize a radio beacon. In our implementation we used heuristics to improve performance without hurting our theoretical guarantees. We modified Algorithm 3 to keep track of the intersection area of all the measurement locations and avoid taking measurements that do not contain the target. We

also modified Algorithm 2 to take a single ND measurement at a higher altitude that covers the entire area required for each step (we triple the height instead of doubling it). Furthermore, if a measurement lies outside the ND region then it acts as a bearing measurement and we use the resulting area (quadrant) to further reduce the measurement intersection area. In order to achieve the same goal both strategies approach the target after localizing it. Performance evaluation was based on mission time difference over 100 simulations.

We generated 60 sets with varying ND region apex angle $\phi \in \{15, 30, 45, 60\}$ deg, target beacon distance $L \in \{150, 300, 600, 1200, 2400\}m$ and for uniformly distributed measurement bearing noise with varying corruption $\alpha \in \{10, 20, 30\}$ deg. Figure 6 presents how much shorter our strategy is when compared with `Localize-Target-on-Plane` for $r^* = 3$ m. For ambiguous measurement locations that can yield both good and bad directionality we assumed we set $\theta = 0$ (no ambiguity), $\theta = 10$ deg and $\theta = 17$ deg (calculated in Section 3). A location in the ambiguous region has 50% chance to detect the ND region. Our strategy performs better as the initial bearing measurement accuracy increases due to Phase 1 ending closer to the center of the ND region. We also observe a decrease in performance as θ increases, which is expected given the need to cover a larger area in which we need more circles and thus more measurements. An example scenario can be seen in Figure 5. These results show that `ND-Region-Landing` can provide shorter flight times when approaching a target beacon by exploiting the special structure of the ND region and our UAV's ability to change height and approach the target from above.

6 Field Experiments

We validate our strategy with a real UAV system and radio beacon. The UAV we used was a multi-rotor DJI Matrice 100 with 3.4 kg takeoff weight, about 12 minutes flight time and a maximum travel speed of 22 m/sec. An RTL-SDR (Software Defined Radio) USB signal receiver was connected to a 3-element Yagi antenna that can sense and record the signal emitted by our beacon. Our radio beacon was the ATS F1800 which transmits a pulse approximately once every two seconds. In Section 3 we calculated the ND region angles with the real data to be $\phi = 17.8$ deg, $\theta = 17.4$ deg.

We placed the beacon 75 m away from the UAV and used the implementation in Section 5 to get the measurement locations. The input values were $\alpha = 15$ deg and $r^* = 7$ m which for $\phi + \theta = 34$ deg requires a minimum altitude of 10 m (chosen for safety). The resulting trajectory (chosen for visualization purposes) and measurement locations can be seen in Figure 7. The UAV detected the ND region at the third measurement at an altitude of 100 m. Then the altitude was reduced and the ND region was re-detected until it was reduced to a radius $\leq r^*$. The final measurement and landing location was 2 m away from the beacon.

7 Conclusion and Future Work

In this work we studied the problem of landing near the source of a radio signal (beacons) with UAVs. Our main contribution is a strategy that exploits a special structure occurring when a UAV approaches a target beacon from above to reduce the flight time required to land

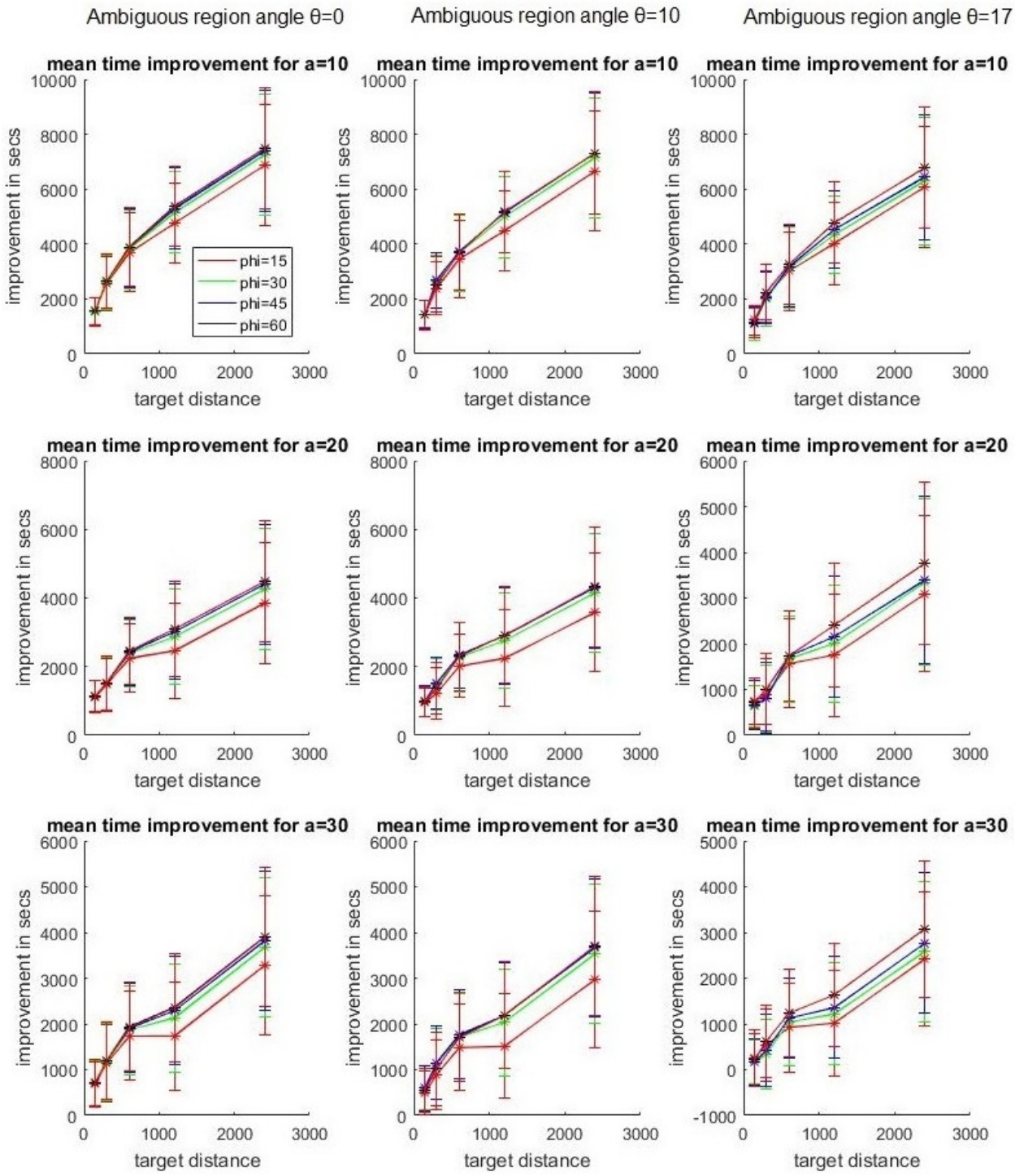

Figure 6: Average mission time improvement of our strategy over `Localize-Target-on-Plane` [11] for varying ND region apex angle ϕ, target beacon distance L (x-axis), bearing measurement noise α. The ambiguous region has size θ and 50% to produce the ND region.

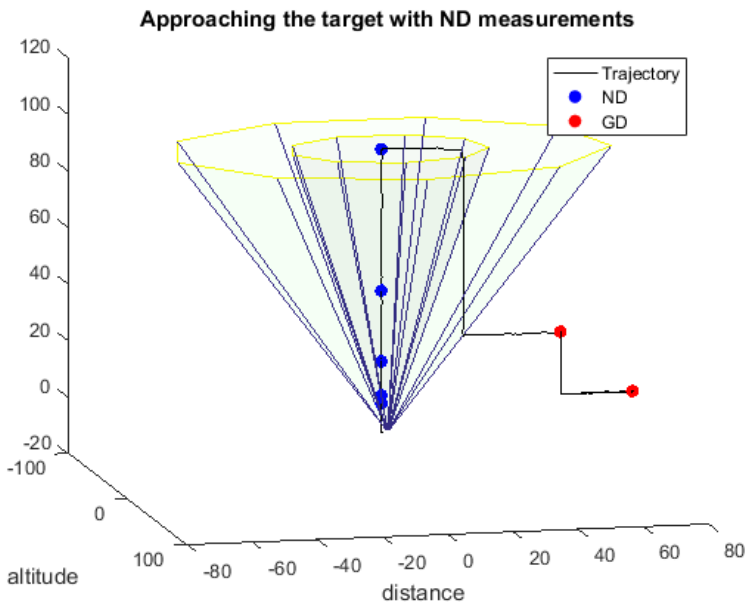

Figure 7: Results from the field experiment for $r^* = 7\ m$, $\phi = 17.8\,\text{deg}$, $\theta = 17.4$. The conic region represents our conic approximation of the ND region. The measurements outside the ND region are colored red (GD) and the measurements inside the ND region are colored blue (ND). The target beacon was at 75m distance away from the initial location.

near it. This is important because current approaches can fail when attempting to localize a target using bearing measurements at a high altitude due to the existence of a conic region above the target inside of which bearing measurements lose directionality: signal recordings in all directions yield similar signal strength (ND region). This way we can detect whether a location is inside the region and the region ground footprint is guaranteed to contain the target. Then we reduce the uncertainty area by decreasing height and re-locating the region. Through simulations comparison with our previous work we demonstrate that we produce shorter localization times and we validate our strategy with a real UAV system.

For our future work there are many venues we can explore. One of the main assumptions of this work is that the target is stationary. What if the target is dynamic and the ND region can move during the measurement acquisition stage? In such cases it may be more advantageous to obtain more measurements at a higher altitude where the ND region is larger. Depending on the distance between the initial starting location and the beacon location Algorithm 1 can result in an altitude that may be undesirable for a practical implementation. Similarly, the desired uncertainty area may require the UAV to fly at very low altitudes which may, again, not be desirable. We would like to provide alternative strategies that can approach and localize the target while reducing the maximum/minimum altitude that needs to be reached. Finally, we would also like to explore alternative strategies to handle the ambiguous region and improve the competitive ratio which can become large.

References

[1] M Heutger and M Kückelhaus. Unmanned aerial vehicle in logistics: a dhl perspective on implications and use cases for the logistics industry. *DHL Customer Solutions & Innovation, Troisdorf, Germany*, 2014.

[2] Alec Momont. Ambulance drone. *Delft University of Technology*, 2016.

[3] Celia Seguin, Gilles Blaquière, Anderson Loundou, Pierre Michelet, and Thibaut Markarian. Unmanned aerial vehicles (drones) to prevent drowning. *Resuscitation*, 127:63–67, 2018.

[4] Jarrod C Hodgson, Shane M Baylis, Rowan Mott, Ashley Herrod, and Rohan H Clarke. Precision wildlife monitoring using unmanned aerial vehicles. *Scientific reports*, 6:22574, 2016.

[5] Matthew Dunbabin and Lino Marques. Robots for environmental monitoring: Significant advancements and applications. *IEEE Robotics & Automation Magazine*, 19(1):24–39, 2012.

[6] Pratap Tokekar, Joshua Vander Hook, and Volkan Isler. Active target localization for bearing based robotic telemetry. In *Intelligent Robots and Systems (IROS), 2011 IEEE/RSJ International Conference on*, pages 488–493. IEEE, 2011.

[7] Haluk Bayram, Joshua Vander Hook, and Volkan Isler. Gathering bearing data for target localization. *IEEE Robotics and Automation Letters*, 1(1):369–374, 2016.

[8] L David Mech. *Handbook of animal radio-tracking*. U of Minnesota Press, 1983.

[9] Kurt VonEhr, Seth Hilaski, Bruce E Dunne, and Jeffrey Ward. Software defined radio for direction-finding in uav wildlife tracking. In *Electro Information Technology (EIT), 2016 IEEE International Conference on*, pages 0464–0469. IEEE, 2016.

[10] Louis Dressel and Mykel J Kochenderfer. Pseudo-bearing measurements for improved localization of radio sources with multirotor uavs. In *2018 IEEE International Conference on Robotics and Automation (ICRA)*, pages 6560–6565. IEEE, 2018.

[11] Haluk Bayram, Nikolaos Stefas, and Volkan Isler. Aerial radio-based telemetry for tracking wildlife. In *2018 IEEE/RSJ International Conference on Intelligent Robots and Systems (IROS)*, pages 4723–4728. IEEE, 2018.

[12] Oliver M Cliff, Robert Fitch, Salah Sukkarieh, Debbie Saunders, and Robert Heinsohn. Online localization of radio-tagged wildlife with an autonomous aerial robot system. In *Robotics: Science and Systems*, 2015.

[13] Haluk Bayram, Nikolaos Stefas, Kazim Selim Engin, and Volkan Isler. Tracking wildlife with multiple uavs: System design, safety and field experiments. In *Multi-Robot and Multi-Agent Systems (MRS), 2017 International Symposium on*, pages 97–103. IEEE, 2017.

[14] Adrien Perkins, Louis Dressel, Sherman Lo, and Per Enge. Antenna characterization for uav based gps jammer localization. In *Proceedings of the 28th International Technical Meeting of The Satellite Division of the Institute of Navigation (ION GNSS+ 2015)*, 2015.

[15] Richard Kershner. The number of circles covering a set. *American Journal of mathematics*, 61(3):665–671, 1939.

[16] CT Zahn and CT Zahn. *Black box maximization of circular coverage*. US Department of Commerce, National Institute of Standards and Technology, 1962.

[17] Hans Melissen. Loosest circle coverings of an equilateral triangle. *Mathematics Magazine*, 70(2):118–124, 1997.

8 Appendix

8.1 Proof of Lemma 2

Proof. From Lemma 1 we need at most 4 circles of radius r_i to cover the entire sector area of a circle with radius $2r_i$ and angle $\alpha < 90\,\text{deg}$. But note that at the previous step $i-1$ we have already covered the area that is covered by the circle center at A and we do not need to cover it again. Thus we only need 3 circles of radius r_i to cover the remaining sector area. Thus, if the center of the ND region is not further away than $2r_i$ visiting the centers of all 3 circles guarantees that we visit at least one point of the ND region. Traveling to the center of each circle requires less than $2r_i$ distance since the circles overlap. Thus, we require at most 3 measurements and 4 steps each of length $\leq 2r_i$ for a total length of $8r_i$. □

8.2 Proof of Theorem 3

Proof. Let the ND region be detected at the k-th step. In order to bound the number of steps k note that detecting the ND region at the k-th step means that $\|CA\| = L > 2r_{k-1} = 2^k r_0$ which implies that $k \leq \log_2(\frac{L}{r_0})$. Thus, during Phase 1 we take at most $3k \leq 4\log_2(\frac{L}{r_0})$ ND measurements. Using Lemma 2 Phase 1 travels at most $8\sum_{j=0}^{k} 2^k r_0 + \|H_k\| = 8r_0(2^{k-1} - 1) + \frac{2^k r_0}{\tan\phi} < r_0 2^k(4 + \frac{1}{\tan\phi}) < 2L(4 + \frac{1}{\tan\phi})$. Since the optimal strategy OPT takes at least one measurement and travel $L - r^*$ (see Section 4.1) the competitive ratio (in terms of travel distance and number of measurements) is $max\left(\frac{2L(4+\frac{1}{\tan\phi})}{L-r^*}, 3\log_2(\frac{L}{r^*})\right)$ for $r^* = r_0$. □

8.3 Proof of Lemma 4

Proof. We define a circle C' centered at A with radius $2r_i$. From Lemma 1 we need at most 7 "small" circles of radius r_i to cover the entire area of a circle with radius $2r_i$. By construction, the ND region cannot be further away than r_i and thus C' contains the center of the ND region. Thus, visiting the centers of all 7 "small" circles guarantees that we visit at least one point of the ND region. The centers of the 6 perimeter "small" circles yield a

hexagon that is inscribed inside the center circle. The length of each side of this hexagon is less than the length of the side of the hexagon inscribed on C' (with radius $2r_i$) which is $4r_i \sin(30^o)$. □

8.4 Proof of Theorem 5

Proof. Lemma 4 gives us the cost of each step and for a total of m steps we travel a total travel distance of $H_k + \sum_{j=0}^{m-1} \frac{12r_k}{2^j} \leq H_k + 12r_k = r_k(12 + \frac{1}{\tan\phi}) \leq 2L(12 + \frac{1}{\tan\phi})$. The analysis for the number of ND measurements follows from Theorem 3 and Lemma 4 and results in $6k \leq 6\log_2(\frac{L}{r^*})$. Thus the competitive ratio for this strategy is $max(\frac{2L(16+\frac{2}{\tan\phi})}{L-r^*}, 9\log_2(\frac{L}{r^*})))$, where $r_0 = r^*$. □